ELSEVIER

Polymer 42 (2001) 7443–7447

polymer

www.elsevier.nl/locate/polymer

Growth shape of isotactic polystyrene crystals in thin films

Ken Taguchi[a,*], Hideki Miyaji[a], Kunihide Izumi[a], Akitaka Hoshino[a], Yoshihisa Miyamoto[b], Ryohei Kokawa[c]

[a]*Department of Physics, Graduate School of Science, Kyoto University, Kyoto 606-8502, Japan*
[b]*Department of Fundamental Sciences, Faculty of Integrated Human Studies, Kyoto University, Kyoto 606-8501, Japan*
[c]*Shimadzu Corporation, Kanagawa 259-1304, Japan*

Received 17 October 2000; received in revised form 19 January 2001; accepted 12 February 2001

Abstract

The crystal growth of isotactic polystyrene (it-PS) is investigated in very thin, 11 nm thick films. The it-PS crystals grown in the thin films show quite different morphology from that in the bulk. With decreasing crystallization temperature, the branching morphology in a diffusion field appears: dendrites and compact seaweed. The branching morphology is formed through a morphological instability caused by the gradient of film thickness around a crystal; the thicker the film thickness, the larger is the lateral growth rate of crystals. Regardless of the morphological change, the growth rate as well as the lamellar thickness depends on the crystallization temperature as predicted by the surface kinetics.

Keywords: Isotactic polystyrene; Crystallization; Thin films

1. Introduction

Recently, crystal growth of polymers in thin films has attracted much attention on morphology and growth rate. Several authors have reported the appearance of diffusion-controlled morphology in polymer thin films. Lovinger and Cais observed the single crystals crystallized from the melt of poly(trifluoroethylene) with branched morphology and discussed the morphology on the basis of the diffusion-limited aggregation [1]. Reiter and Sommer investigated the crystallization of poly(ethylene oxide) in quasi-two-dimensional monolayers and suggested that a diffusion field caused finger-like branched patterns observed [2]; Sakai et al. reported the diffusion-limited crystal growth of poly(ethylene terephthalate) in thin films [3].

On the other hand, when isotactic polystyrene (it-PS) is crystallized from the melt in thin films down to 20 nm, the crystal has shown the same morphological change with crystallization temperature. Above 200°C, the crystals grown are hexagonal plates, rounded hexagonal plates around 195°C, circular discs at 180°C (Fig. 1), and below 170°C, two-dimensional spherulites [4,5]. Although the morphology is unchanged, the growth rates have been observed to decrease in thin films. The film thickness dependence of the growth rate was expressed by the following equation:

$$\frac{G(d)}{G(\infty)} = 1 - \frac{a}{d}, \tag{1}$$

where $G(d)$ is the growth rate in a film of thickness d, $G(\infty)$ is the growth rate in the bulk and a is a constant of about 6 nm [5]. The constant a was independent of crystallization temperatures, molecular weight and substrate material.

In the present paper, we report the morphology, growth rate and crystal thickness of it-PS crystals grown in ultrathin films, the thickness of which is less than the radius of gyration of a polystyrene molecule in the melt. In particular, the morphology will be discussed in the light of morphological instability in a diffusion field specific to thin polymer films, and compared with numerical simulations of crystal growth by Saito and Ueta [6], which took account of both surface kinetic process and diffusion process.

2. Experimental

The it-PS used in this study was purchased from Polymer Laboratory ($M_w = 590\,000$, $M_w/M_n = 3.4$, tacticity: 97% isotactic triad). This molecular weight corresponds to 22 nm in radius of gyration of a polystyrene molecule in the melt. Ultrathin films of it-PS were prepared on a carbon-evaporated glass slide by spin coating at 4000 rpm; amorphous it-PS

* Corresponding author. Tel./fax: +81-75-753-3754.
E-mail address: taguchi@scphys.kyoto-u.ac.jp (K. Taguchi).

0032-3861/01/$ - see front matter
PII: S0032-3861(01)00215-4

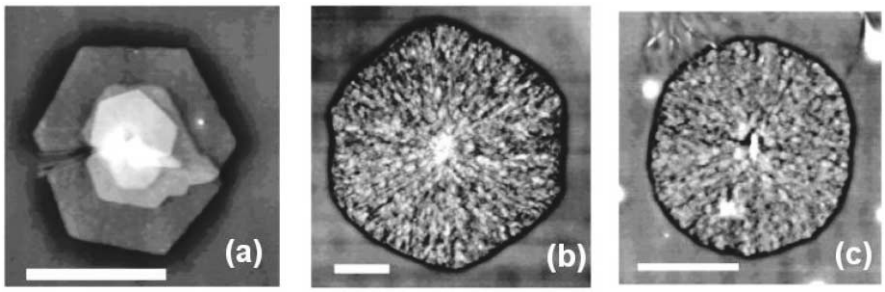

Fig. 1. AFM images of it-PS crystals grown in films thicker than 50 nm at (a) 210°C for 2 h 45 min, (b) 195°C, 1 h, and (c) 180°C, 20 min. Scale bars represent 5 μm. These crystals consist of not single lamella but many overgrowth lamellae.

films with uniform thickness of about 11 nm were obtained with use of a 0.4 wt% cyclohexanone solution. The thickness of the film is determined by an atomic force microscope (AFM) (SHIMADZU SPM-9500J). The films thereby obtained were crystallized isothermally at several temperatures, 180, 190, 195, 200, 205 and 210°C for a certain period of time in a hot stage (Mettler FP800). Before crystallization, the films were melted at 250°C for 3 min, quenched to room temperature much lower than the glass transition temperature, T_g (90°C), and immediately elevated to a crystallization temperature. The lateral growth rate was determined by in situ differential-contrast optical microscopy. Detailed morphology and structure of the crystals were investigated by the AFM and a transmission electron microscope (TEM) (JEOL 1200EX II) at room temperature.

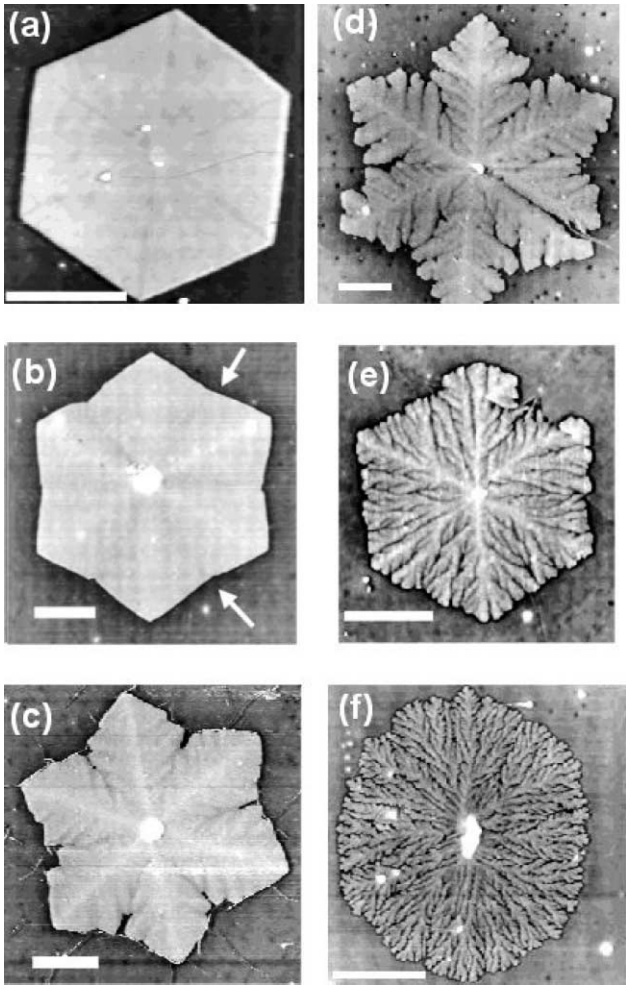

Fig. 2. AFM images of it-PS crystals grown in 11 nm thick film at (a) 210°C for 4 h, (b) 205°C, 4 h, 4 h (c) 200°C, 4 h, (d) 195°C, 3 h, (e) 190°C, 1 h, and (f) 180°C, 1 h. Scale bars represent 5 μm. The arrows in (b) show the reentrant sites, where the growth rates decrease during growth.

3. Results

Fig. 2 shows the AFM images of it-PS crystals grown at several crystallization temperatures in 11 nm thick films. It is to be noted that 11 nm is about a half of the radius of gyration of the molecules. The fact that these crystals can be observed by AFM necessitates the protrusion of crystals from the surface of the surrounding amorphous it-PS. Indeed, in polymer crystallization in thin films, amorphous region close to the growth interface is always thinner by several nanometers than the region far from the interface. The surface of a lamellar crystal, including both the upper side and lateral growth front, is covered by an amorphous layer a few nm in thickness [4,7–9]. A schematic view of the cross-section is drawn in Fig. 3. At 210°C, the morphology of the crystal is a hexagon with the 110 facets same as in the bulk. Below 210°C, however, the crystals were found to show morphology different from that in the bulk. At 205°C, the 110 facets are no longer flat but have reentrant corners to form a star-like shape. Side branches begin to appear at 200°C and appears as a dendrite similar to a snowflake at 195°C. At 190°C, a dendrite has a number of side

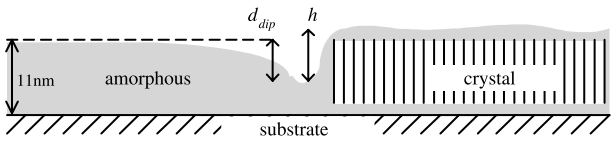

Fig. 3. A schematic view of the cross-section. h is the height difference between the upper surface of the crystals and the bottom of the concave amorphous surface near the crystal growth face, d_{dip} is the depth of the concave region. The vertical scale is magnified about 100 times compared with the horizontal scale.

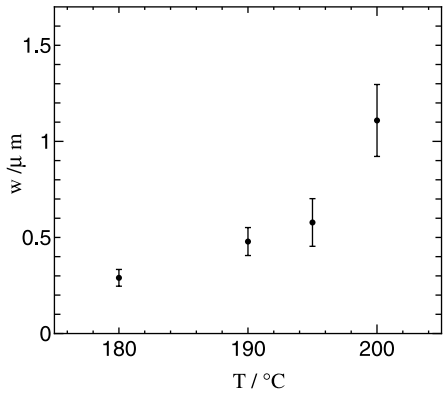

Fig. 4. The mean width of branches w vs. crystallization temperature T in it-PS 11 nm thick films.

branches, and the crystal still has sixfold symmetry. Below 180°C, we can observe the splitting of growing tips and many irregular branches to form the morphology similar to the compact seaweed (CS) [10] or dense branching morphology (DBM) [11] with a circular and convex envelope. The mean width of branches, w, measured directly from AFM images, decreases with decreasing crystallization temperatures as shown in Fig. 4. The electron diffraction pattern from a crystal grown at 180°C is shown in Fig. 5 with its bright field image. Although there are many irregular branches, the pattern reveals that this crystal has a single crystallographic orientation with the chain axis perpendicular to the film surface. In fact, all the crystals in Fig. 2 were single crystals. With decreasing crystallization temperatures, the morphology of the it-PS single crystals in ultrathin films, therefore, changes from a nucleation-controlled faceted hexagonal plate to the branching morphology observed in the crystal growth in a diffusion field.

In polymer crystallization, important aspects besides morphology are the thickness of a lamellar crystal and the lateral growth rate [12]. The thickness of each crystal is almost constant during growth as revealed by the uniform contrast in the AFM image of crystal surfaces (Fig. 2). Since amorphous layers cover the upper and lateral surfaces of crystals and should also exist between the crystals and the

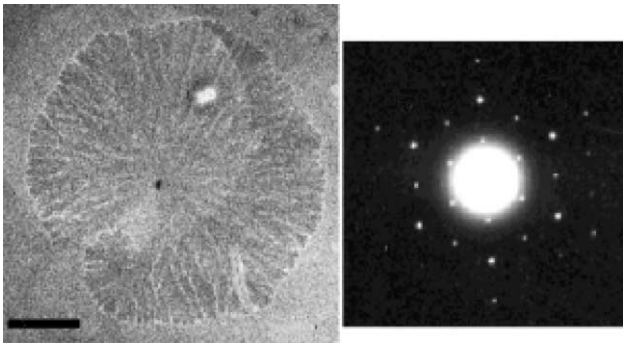

Fig. 5. Bright field image and electron diffraction pattern of an it-PS crystal grown at 180°C in ultrathin film. Scale bar is 2 μm.

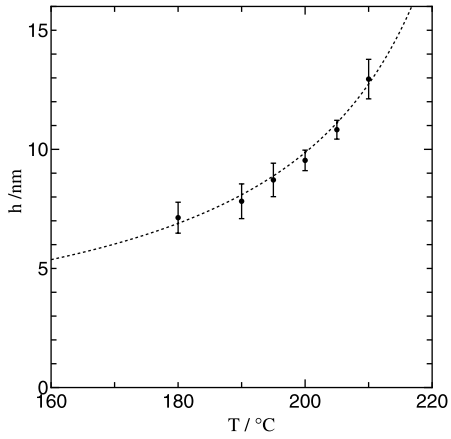

Fig. 6. The height difference h in Fig. 3 vs. crystallization temperature T. The dotted curve shows the theoretical temperature dependence of the lamellar thickness l_g^* [12]: $l_g^* = [2\sigma_e T_m^0/\Delta h_f(\Delta T)] + \delta l$; $\delta l = (kT/2b\sigma)((4\sigma/a) + \Delta f)/((2\sigma/a) + \Delta f)$, $\sigma = 7.65$ ergs/cm^2, $\sigma_e = 34.8$ ergs/cm^2, $\Delta h_f = 9.40 \times 10^8$ ergs/cm^3, $T_m^0 = 242$°C $a = 6.3$ Å, $b = 10.9$ Å.

substrate [8], it is difficult to determine the absolute value of the lamellar thickness. However, as shown in Fig. 3, the height difference h may be a relative measure of the thickness since the amorphous layers covering the crystals are considerably thin compared with lamellar thickness and the depth of concave region, d_{dip}, has an almost constant value of several nanometers in ultrathin films. The height differences measured increased with the crystallization temperature, agreeing well with the theoretical curve of lamellar thickness [12] as shown in Fig. 6. This result suggests that crystallization temperature dependence of the lamellar thickness in ultrathin films is almost the same as in the bulk [13]. For the growth rate determined by the time development of the separation of the farthest tip r_{tip} from the center of the crystal (Fig. 7), the rate was found to be constant during growth (linear growth) and was about 5/11 of those in the bulk at each crystallization temperature (Fig. 8), agreeing well with Eq. (1) for $d = 11$ nm and

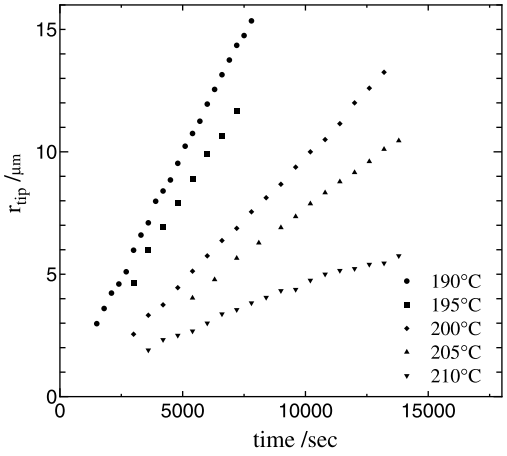

Fig. 7. Time developments of r_{tip} of an it-PS crystal in 11 nm thick films at each crystallization temperature.

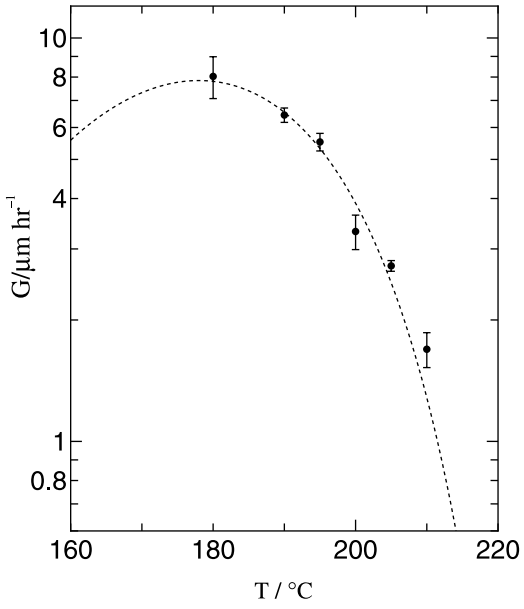

Fig. 8. Growth rates vs. crystallization temperatures in 11 nm thick films. The dotted curve shows the growth rate in the bulk multiplied by a factor 5/11.

$a = 6$ nm. As for the reentrant site of the crystal between the farthest tips shown by the arrows in Fig. 2(b), on the other hand, the growth rate was not constant but decreased during growth and the film thickness in front of the reentrant site decreases with time. It should be noted, however, that the lamellar crystal thickness is almost constant throughout the crystal including the reentrant site with the different growth rate. Consequently, the lamellar thickness and the linear growth rate at the growing tip in the ultrathin films depend on the crystallization temperature as in the bulk. Hence, the surface kinetics [12,14,15] of the crystallization in ultrathin films is the same as that in the bulk regardless of the drastic morphological change.

4. Discussion

According to the theory of crystal growth, dendrites and CS can appear in the crystal growth in a diffusion field. When a part of the flat interface grows faster than the other by some fluctuation, the advanced part can grow faster owing to a gradient (e.g. of concentration) in the diffusion field, and the deformation is enhanced. Hence, the flat interface becomes unstable, resulting in dendrites or CS. The morphology of it-PS crystals grown in ultrathin films below 205°C, therefore, suggests that a diffusion process plays an important role in the crystal growth. In fact, the morphological change with increasing supercooling or driving forces similar to the present study has been reported in both experiment and simulation on crystal growth in a diffusion field [6,16–19]. For example, in the growth of snow crystals, both a diffusion process and a surface kinetic process are closely reflected in the variety of growth shape [19]. Saito and Ueta performed the Monte Carlo (MC) simulation on the crystal growth in a diffusion field [6] and found the morphological transition from a polygon through a dendrite to CS with increasing driving force, which is very similar to our result. A further important point in their study is that those crystals show a linear growth, and surface kinetics controls the growth until morphological transition to CS occurs. Hence, in the crystallization of it-PS in ultrathin films, the surface kinetics, which determines the growth rate and the lamellar thickness, keeps working at the growth tip while the morphology is controlled by diffusion process.

Here, we must ask a question: what kind of diffusion field causes the instability in the present case? The diffusion field is generally either that of concentration or temperature with a gradient at growth face; the gradient causes the instability of flat growth faces to give rise to dendrites or DBM depending on supersaturation or supercooling and the strength of anisotropy in surface free energy. However, in the crystallization of polymers, the growth rate is so slow that the thermal diffusion length is much larger than crystal size, and hence, no appreciable temperature gradient exists [20]; we can neglect the effect of thermal diffusion. In the melt growth, no concentration gradient exists other than that of any kind of impurity. However, we need not take into consideration even the effect of impurity diffusion because no morphological instability is observed in the crystal growth in the thicker films in spite of much higher growth rates.

Detailed inspection of the AFM images in Fig. 2 elucidates the gradient of thickness of melt around a crystal; the thickness of melt increases gradually with separation from the crystal edge to surrounding melt. The gradient is formed owing to the protrusion of a crystal from the surrounding melt [7]. This gradient makes self-diffusion field in front of growing crystals. Since the thickness in thin films is proportional to the amount of polymer segment per unit area, the thickness of melt, d, can correspond to the concentration; we can recognize this morphological instability on the analogy of that of the crystal growth from solutions. Therefore, it must be this gradient of film thickness around the crystal that introduces the instability. The effect of this gradient on the growth rate may be related to the film thickness dependence of the growth rate (Eq. (1)). However, the detail of this relation is yet to be discussed. The film thickness in the previous study [5] was above 20 nm and much thicker than the depletion of the thickness around a crystal of several nanometers, and hence, the effect of the gradient of thickness on the growth rate was so small that no morphological instability was observed.

Lastly, we consider one of the main structures of branching morphology, the separation between branches w (Fig. 4). The characteristic length of diffusion-controlled growth is generally given by the stability length $\lambda_s = 2\pi\sqrt{d_0 l_D}$, where d_0 is a capillary length and l_D, a diffusion length [21,22]. Indeed, the occurrence of spherulites, which consist of

stacking lamellae, was accounted for with the diffusion-controlled growth, and their characteristic dimension was predicted to be scaled with λ_s [23]. In the MC simulation mentioned above, on the other hand, the structure of dendrites is characterized by the diffusion length l_D. In either case, the change in l_D with decreasing temperatures allows us to predict the qualitative change in characteristic length. The diffusion length is given by $l_D = 2D/G$, where D is the diffusion coefficient and G is the growth rate; in the present experiment of melt crystallization, we assume that D represents the self-diffusion coefficient of polymer chains. In the range of crystallization temperature investigated, the growth rate increases rapidly with decreasing crystallization temperatures (Fig. 5), while the diffusion coefficient generally decreases with decreasing temperatures, and hence, l_D decreases rapidly with decreasing crystallization temperatures, agreeing with the experimental result (Fig. 4).

5. Conclusions

We have clearly shown that the morphology of it-PS crystals grown in ultrathin films changes from the faceted morphology to that in the diffusion field; the lateral growth interface becomes unstable with the increasing in supercooling. This morphological instability is considered to result from the gradient of film thickness around the crystal; the formation of gradient is specific in polymer crystallization in thin films. The growth rates and the lamellar thickness show that the surface kinetics keeps working on the crystallization in ultrathin films while the morphology is controlled by diffusion process.

Acknowledgements

This work was supported by Grant-in-Aid for Science Research on Priority Areas, “Mechanism of Polymer Crystallization” (no. 12127204) and Grant-in-Aid for Exploratory Research no. 12874048 from The Ministry of Education, Science, Sports and Culture.

References

[1] Lovinger AJ, Cais RE. Macromolecules 1984;17:1939–45.
[2] Reiter G, Sommer J-U. Phys Rev Lett 1998;17:3771–4.
[3] Sakai Y, Imai M, Kaji K, Tsuji M. J Cryst Growth 1999;203:244–54.
[4] Izumi K, Gan P, Hashimoto M, Toda A, Miyaji H, Miyamoto Y, Nakagawa Y. In: Nishinaga T, Nishioka K, Harada J, Sasaki A, Takei H, editors. Advances in the understanding of crystal growth mechanisms. Amsterdam: Elsevier Science, 1997. p. 337.
[5] Sawamura S, Miyaji H, Izumi K, Sutton SJ, Miyamoto Y. J Phys Soc Jpn 1998;67:3338–41.
[6] Saito Y, Ueta T. Phys Rev A 1989;40:3408–19.
[7] Izumi K, Gan P, Toda A, Miyaji H, Hashimoto M, Miyamoto Y, Nakagawa Y, Jpn J Appl Phys 1994;33:1628–30.
[8] Sutton SJ, Izumi K, Miyaji H, Fukao K, Miyamoto Y. Polymer 1996;37:5529–32.
[9] Sutton SJ, Izumi K, Miyaji H, Miyamoto Y, Miyashita S. J Mater Sci 1997;32:5621–7.
[10] Brener E, Müller-Krumbhaar H, Temkin D. Europhys Lett 1992;17:535–40.
[11] Ben-Jacob E, Deutscher G, Garik P, Goldenfeld ND, Lereath Y. Phys Rev Lett 1986;57:1903–06.
[12] Hoffman JD, Davis GT, Lauritzen JI. In: Hannary NB, editor. Treatise on solid state chemistry, 3. New York: Plenum Press, 1976. Chap. 7.
[13] Miyamoto Y, Tanzawa Y, Miyaji H, Kiho H. J Phys Soc Jpn 1989;58:1879–82.
[14] Saddler DM, Gilmer GH. Phys Rev B 1988;38:5684–93.
[15] Doye JPK. Polymer 2000;41:8857–67.
[16] Ovsienko DE, Alfintsev GA, Maslov VV. J Cryst Growth 1974;26:233–8.
[17] Oswald P, Malthête J. Pelcé P. J Phys Fr 1989;50:2121–38.
[18] Kobayashi R. Physica D 1993;63:410–23.
[19] Yokoyama E, Kuroda T. Phys Rev A 1990;41:2038–49.
[20] Toda A. Faraday Disc 1993;95:129–43.
[21] Mullins WW, Sekerka RF. J Appl Phys 1964;35:444–51.
[22] Keith HD, Padden Jr FJ. J Appl Phys 1963;34:2409–21.
[23] Goldenfeld N. J Cryst Growth 1987;84:601–8.